AIAA SciTech Forum
8–12 January 2018, Kissimmee, Florida
2018 AIAA/ASCE/AHS/ASC Structures, Structural Dynamics, and Materials Conference
10.2514/6.2018-0051

Controller Design and Validation of Dynamic Response for Full-Scale Helicopter Flight Simulator at CCSU

David J. Broderick[*], Fu-Shang (John) Wei[†], and Jeremy Hopwood[‡]
School of Engineering, Science, and Technology
Central Connecticut State University
New Britain, Connecticut, 06050

A research team comprised of students and faculty from Central Connecticut State University's (CCSU) School of Engineering, Science, and Technology has begun the design, production, and testing of a full-scale helicopter flight simulator with a moving platform. This paper will present the system identification, controller tuning and validation, and comparison of simulator dynamics against available helicopter dynamic models during typical flight maneuvers. The purposes for conducting this research include: i) to build a fully functional flight simulator that can be used as a test bed for students research projects; ii) to apply theoretical lessons of control of dynamic systems to a real, tangible electromechanical system; iii) to provide students with hands-on experience on how to design and fly a helicopter. CCSU students have built and programed all of the mechanical and electrical systems. The basic design weight for the simulator is 300 lbs force applied to the pilot seat. The structures are designed to have enough strength to sustain a maximum of 3g and a minimum -1g flight conditions. There are three actuators in place that can be used to rotate the platform in the pitching, rolling, and yawing directions. All electrical systems were designed, fabricated, and assembled by CCSU students. The controller was designed and implemented by the students and faculty of CCSU.

Nomenclature

M_0	=	moment about point 0
H_0	=	angular momentum about point 0
$[I]$	=	platform moment of inertia tensor
$[\theta]$	=	platform angle vector
φ	=	platform roll angle
θ	=	platform pitch angle
ψ	=	platform yaw angle
$F_{\{R,P,Y\}}$	=	force applied to platform by {Roll, Pitch, Yaw} motor
$d_{\{R,P,Y\}}$	=	distance from application of {Roll, Pitch, Yaw} force to point 0
m	=	mass of platform
g	=	gravitational acceleration
$\bar{z}$	=	distance from point 0 to centroid of platform

[*]Teaching Faculty, Ph.D., Computer Electronics & Graphics Technology Department, CCSU.
[†]Teaching Faculty, D.Sc., Engineering Department, CCSU.
[‡]Student, Mechanical Engineering, CCSU.

V_a	=	motor input voltage
L_a	=	armature circuit inductance
R_a	=	armature circuit resistance
k_t	=	motor torque constant
k_b	=	motor back *emf* constant
T_m	=	armature torque
T_L	=	motor load torque
T	=	motor torque
J_m	=	motor polar moment of inertia
c_m	=	motor damping
k_g	=	rotational to linear gear ratio
$G_{\{\varphi,\theta,\psi\}}$	=	system identified for {Roll, Pitch, Yaw}
K_p	=	proportional gain
K_i	=	integral gain
K_d	=	derivative gain
τ_f	=	time constant of the first-order derivative filter

I. Introduction

A helicopter flight simulator is a machine that can be used as a training tool to aid in the development of the helicopter pilot's skill. This tool can replace an actual aircraft during pilot training, thereby greatly reducing the training cost and significantly enhancing pilot flight safety.[1–15] With these cost saving and flight safety benefits in mind, a student faculty research team at Central Connecticut State University (CCSU) School of Engineering, Science, and Technology has begun the design, production, and testing of a full-scale helicopter flight simulator with a moving platform that simulates a real helicopter in flight.[14–19] This student-led effort will begin to validate the performance of the electro-mechanical system with regards to its use as a helicopter flight simulator.[15–25]

I.A. Background

Figure 1 presents the full-scale CCSU flight simulator built by student and faculty members. The mechanical design that depended on off-the-shelf hardware was previously presented.[26] Several groups have contributed to this work over many semesters. The project began with a fixed-base simulator using the X-plane® software. The team used this commercially available simulation software in conjunction with flight controls and a projector to train university students during the CCSU summer helicopter training program. Subsequent groups of students designed a mechanically actuated platform to allow the simulator to roll, pitch, and yaw. Other groups have improved the transient response of the system by developing an 8 to 1 pulley system, added potentiometers to provide feedback to the controller, improved the yaw angle from ±25° to ±45°, and developed a heads-up-display (HUD). The most recent group of students redesigned and programmed the electrical control system.[27]

The current work focuses on the tuning and characterization of the controller and resulting dynamic performance of the simulator. The goals for this work are:

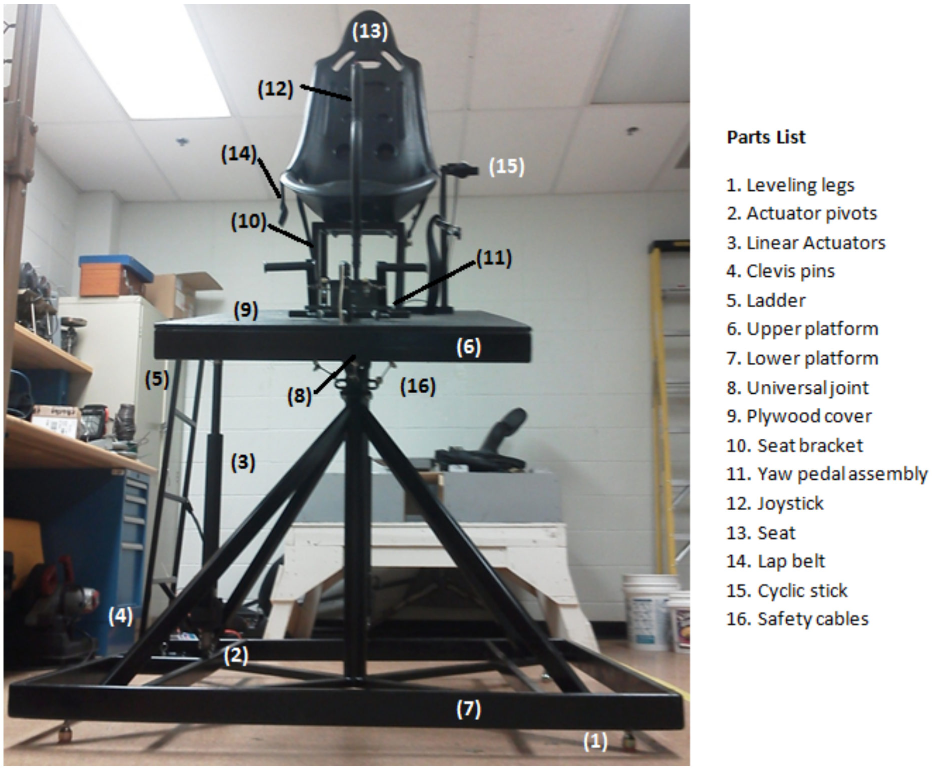

Figure 1. CCSU flight simulator with key parts labeled.

i) Identify the open-loop response of simulator platform for use in controller design

ii) Choose a controller tuning that will satisfy the requirement that the platform accurately follow a simulation of helicopter dynamics

iii) Validate the dynamic performance of the simulator using standard flight maneuvers in the X-plane® simulation software.

The previous implementation of the controller was a simple proportional control with no attention paid to tracking error. As expected, the performance did not track the reference provided in Fig. 2.

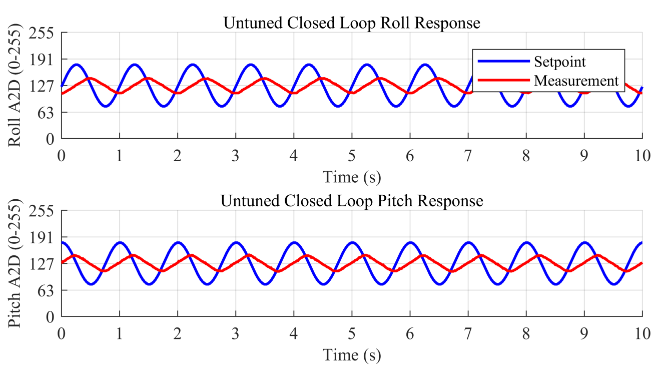

Figure 2. Tracking error with previous controller architecture and tuning

II. System Identification

A model of the system was developed and identified in order to understand the dynamic response of the simulator. The model was then used to determine the three gains to be implemented in a PID controller. The model presented in the following section describes the mechanical system without regard for the electrical system controlling it. Later sections will consider the electrical dynamics.

II.A. Platform Dynamic Modeling

The flight simulator platform was modeled as a rigid body rotating about a fixed-point in three dimensional space. The relationship between the sum of the external moments and the angular impulse was used to develop an understanding of model order. That relationship is stated as

$$\sum M_0 = \dot{H}_0 \tag{1}$$

The angular momentum can be written as the product of the moment of inertia and the angular velocity. In the case of generalized rigid body motion this is extended to be the product of the moment of inertia tensor and the angular velocity vector.

$$\sum M_0 = \frac{\partial}{\partial t}([I][\dot{\theta}]) \tag{2}$$

Expanding the time derivative gives

$$\sum M_0 = [I][\ddot{\theta}] + [\dot{\theta}] \times ([I][\dot{\theta}]) \tag{3}$$

The moments on the platform include the moments due to the force applied by the motors and the weight of the platform. The vector cross product is generalized as the following matrix product.

$$\begin{bmatrix} F_R d_R \cos|\varphi| + mg\bar{z}\sin\varphi \\ F_P d_P \cos|\theta| - mg\bar{z}\sin\theta \\ F_Y d_Y \cos|\psi| \end{bmatrix} = \begin{bmatrix} I_{xx} & I_{xy} & I_{xz} \\ I_{xy} & I_{yy} & I_{yz} \\ I_{xz} & I_{yz} & I_{zz} \end{bmatrix} \begin{bmatrix} \ddot{\varphi} \\ \ddot{\theta} \\ \ddot{\psi} \end{bmatrix} + \begin{bmatrix} 0 & -\dot{\psi} & \dot{\theta} \\ \dot{\psi} & 0 & -\dot{\varphi} \\ -\dot{\theta} & \dot{\varphi} & 0 \end{bmatrix} \begin{bmatrix} I_{xx} & I_{xy} & I_{xz} \\ I_{xy} & I_{yy} & I_{yz} \\ I_{xz} & I_{yz} & I_{zz} \end{bmatrix} \begin{bmatrix} \dot{\varphi} \\ \dot{\theta} \\ \dot{\psi} \end{bmatrix} \tag{4}$$

The above equation is rearranged and partially expanded to become

$$\begin{bmatrix} \ddot{\varphi} \\ \ddot{\theta} \\ \ddot{\psi} \end{bmatrix} = \begin{bmatrix} I_{xx} & I_{xy} & I_{xz} \\ I_{xy} & I_{yy} & I_{yz} \\ I_{xz} & I_{yz} & I_{zz} \end{bmatrix}^{-1} \begin{bmatrix} F_R d_R \cos|\varphi| + mg\bar{z}\sin\varphi + \dot{\varphi}(I_{xy}\dot{\psi} - I_{xz}\dot{\theta}) + \dot{\theta}(I_{yy}\dot{\psi} - I_{yz}\dot{\theta}) + \dot{\psi}(I_{yz}\dot{\psi} - I_{zz}\dot{\theta}) \\ F_P d_P \cos|\theta| - mg\bar{z}\sin\theta - \dot{\varphi}(I_{xx}\dot{\psi} - I_{xz}\dot{\varphi}) - \dot{\theta}(I_{xy}\dot{\psi} - I_{yz}\dot{\varphi}) - \dot{\psi}(I_{xz}\dot{\psi} - I_{zz}\dot{\varphi}) \\ F_Y d_Y \cos|\psi| + \dot{\varphi}(I_{xx}\dot{\theta} - I_{xy}\dot{\varphi}) + \dot{\theta}(I_{xy}\dot{\theta} - I_{yy}\dot{\varphi}) + \dot{\psi}(I_{xz}\dot{\theta} - I_{yz}\dot{\varphi}) \end{bmatrix} \tag{5}$$

As seen in Eq. (5), the equations of motion are non-linear and contain a large number of parameters that would need to be identified, mainly the components of the moment of inertia tensor. This poses a problem in the process of system identification in that a high order of excitation would be required to properly estimate the model parameters.

II.B. Platform Linearization Through Basic Assumptions

In order to simplify the non-linear equations of motion and get to a linear approximation, the products of inertia, I_{xy}, I_{yz}, and I_{xz}, were assumed to be zero. Eq. (5) simplifies to

$$\begin{bmatrix} \ddot{\varphi} \\ \ddot{\theta} \\ \ddot{\psi} \end{bmatrix} = \begin{bmatrix} I_{xx} & 0 & 0 \\ 0 & I_{yy} & 0 \\ 0 & 0 & I_{zz} \end{bmatrix}^{-1} \begin{bmatrix} F_R d_R \cos|\varphi| + mg\bar{z}\sin\varphi + \dot{\theta}\dot{\psi}(I_{yy} - I_{zz}) \\ F_P d_P \cos|\theta| - mg\bar{z}\sin\theta - \dot{\varphi}\dot{\psi}(I_{xx} - I_{zz}) \\ F_Y d_Y \cos|\psi| + \dot{\varphi}\dot{\theta}(I_{xx} - I_{yy}) \end{bmatrix} \tag{6}$$

Further expansion of the product yields

$$\begin{bmatrix} \ddot{\varphi} \\ \ddot{\theta} \\ \ddot{\psi} \end{bmatrix} = \begin{bmatrix} \frac{1}{I_{xx}}(F_R d_R \cos|\varphi| + mg\bar{z}\sin\varphi + \dot{\theta}\dot{\psi}(I_{yy} - I_{zz})) \\ \frac{1}{I_{yy}}(F_P d_P \cos|\theta| - mg\bar{z}\sin\theta - \dot{\varphi}\dot{\psi}(I_{xx} - I_{zz})) \\ \frac{1}{I_{zz}}(F_Y d_Y \cos|\psi| + \dot{\varphi}\dot{\theta}(I_{xx} - I_{yy})) \end{bmatrix} \tag{7}$$

This solution can be expressed in non-linear state space with the following defined states

$$\mathbf{x} = \begin{bmatrix} x_1 \\ x_2 \\ x_3 \\ x_4 \\ x_5 \\ x_6 \end{bmatrix} = \begin{bmatrix} \varphi \\ \dot{\varphi} \\ \theta \\ \dot{\theta} \\ \psi \\ \dot{\psi} \end{bmatrix} \tag{8}$$

leading to the state space representation of the model stated as

$$\dot{\mathbf{x}} = \begin{bmatrix} \dot{x_1} \\ \dot{x_2} \\ \dot{x_3} \\ \dot{x_4} \\ \dot{x_5} \\ \dot{x_6} \end{bmatrix} = \begin{bmatrix} x_2 \\ \frac{1}{I_{xx}}(F_R d_R \cos|x_1| + mg\bar{z}\sin x_1 + x_4 x_6(I_{yy} - I_{zz})) \\ x_4 \\ \frac{1}{I_{yy}}(F_P d_P \cos|x_3| - mg\bar{z}\sin x_3 - x_2 x_6 \psi(I_{xx} - I_{zz})) \\ x_6 \\ \frac{1}{I_{zz}}(F_Y d_Y \cos|x_5| + x_2 x_4(I_{xx} - I_{yy})) \end{bmatrix} \tag{9}$$

In order to remove the non-linearity, it can be assumed that $mg\bar{z}\sin x_1 >> x_4 x_6(I_{yy} - I_{zz})$ and $mg\bar{z}\sin x_3 >> x_2 x_6(I_{xx} - I_{zz})$. Furthermore, the platform rotation angles are assumed to be small, and therefore approximations can be made that $\sin\theta = \theta$ and $\cos\theta = 1$. These assumptions yield the following linear state space:

$$\dot{\mathbf{x}} = \begin{bmatrix} \dot{x}_1 \\ \dot{x}_2 \\ \dot{x}_3 \\ \dot{x}_4 \\ \dot{x}_5 \\ \dot{x}_6 \end{bmatrix} = \begin{bmatrix} 0 & 1 & 0 & 0 & 0 & 0 \\ \frac{mg\bar{z}}{I_{xx}} & 0 & 0 & 0 & 0 & 0 \\ 0 & 0 & 0 & 1 & 0 & 0 \\ 0 & 0 & \frac{mg\bar{z}}{I_{yy}} & 0 & 0 & 0 \\ 0 & 0 & 0 & 0 & 0 & 1 \\ 0 & 0 & 0 & 0 & 0 & 0 \end{bmatrix} \begin{bmatrix} x_1 \\ x_2 \\ x_3 \\ x_4 \\ x_5 \\ x_6 \end{bmatrix} + \begin{bmatrix} \dot{x}_1 \\ \dot{x}_2 \\ \dot{x}_3 \\ \dot{x}_4 \\ \dot{x}_5 \\ \dot{x}_6 \end{bmatrix} = \begin{bmatrix} 0 & 0 & 0 \\ \frac{d_R}{I_{xx}} & 0 & 0 \\ 0 & 0 & 0 \\ 0 & \frac{d_P}{I_{yy}} & 0 \\ 0 & 0 & 0 \\ 0 & 0 & \frac{d_Y}{I_{zz}} \end{bmatrix} \begin{bmatrix} F_R \\ F_P \\ F_Y \end{bmatrix} \quad (10)$$

The approximate model developed here can now be applied to the complete electromechanical system under consideration.

II.C. Electromechanical System to be Identified

The block diagram for the electromechanical system for a single Eulerian angle (roll) is shown in Figure 3. This block diagram reduces to a fifth order system with one zero. The poles of the platform rotational

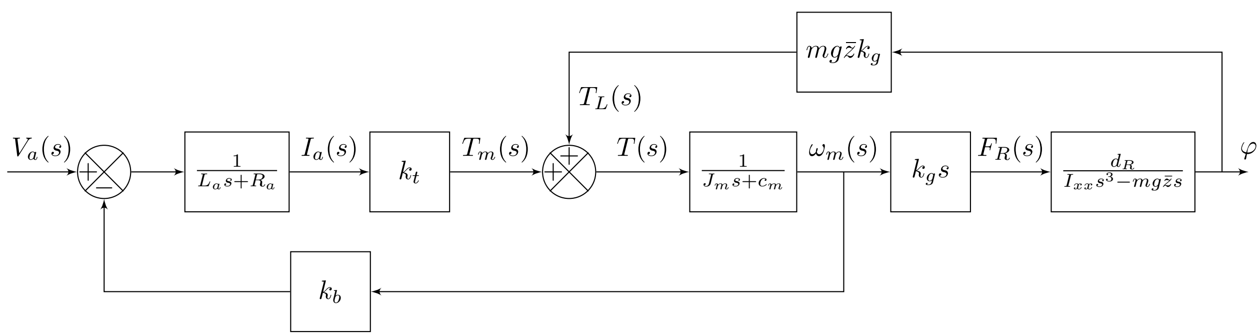

Figure 3. Electromechanical system block diagram

system are assumed to be dominant when considered with regard to the poles from the armature circuit and motor dynamics ($L_a = 0$ and $J_m = 0$). This reduces the model to a system of three poles and one zero represented by

$$\frac{\varphi}{V_a} = \frac{a_1 s + a_0}{b_3 s^3 + b_2 s^2 + b_1 s + b_0} \quad (11)$$

The stated assumptions allow identification of the reduced order approximation using a lower order of excitation.

II.D. Model Form

A discrete ARX model of the same order estimates the sampled data recorded during identification. The discrete model is stated as

$$y[n] = b_0 x[n] + b_1 x[n-1] + b_2 x[n-2] + b_3 x[n-3] + a_1 y[n-1] \quad (12)$$

where $y[n]$ is the output of the model, ie∼pitch, roll, or yaw of the simulator platform as measured from a potentiometer mounted on each actuator. The measurement is performed by an eight bit analog to digital converter. The input to the model, $x[n]$, is a single unsigned byte ranging from 0 to 255. This input byte is converted to a duty cycle by the microcontroller and subsequently filtered before being passed to the Hbridge. Figure 4 shows the individual components of the system that are lumped into the black box model.

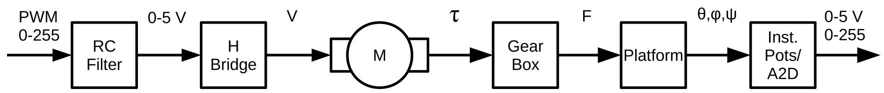

Figure 4. Open loop system architecture of CCSU flight simulator

Sampled data from this system detailed in the next section was used to estimate the parameters described in Eq. (12).

II.E. Model Training and Validation

A chirp was chosen as the excitation signal for collection of training data. During data collection an asymmetry in the platform was observed. The motor dead-band was the primary source of this asymmetry as confirmed by simple jog tests with varying duty cycles applied to the motor. Data was collected to characterize the response of the platform in both the positive and negative directions for all there Eulerian angles. This behavior is a clear indication that linear approximation of the system is, in fact, not an accurate model of the system. However, this nonlinearity can be treated as a disturbance and will be rejected by the closed loop system. Figures 5 through 7 show the open loop responses as well as the input signals used in parameter estimation.

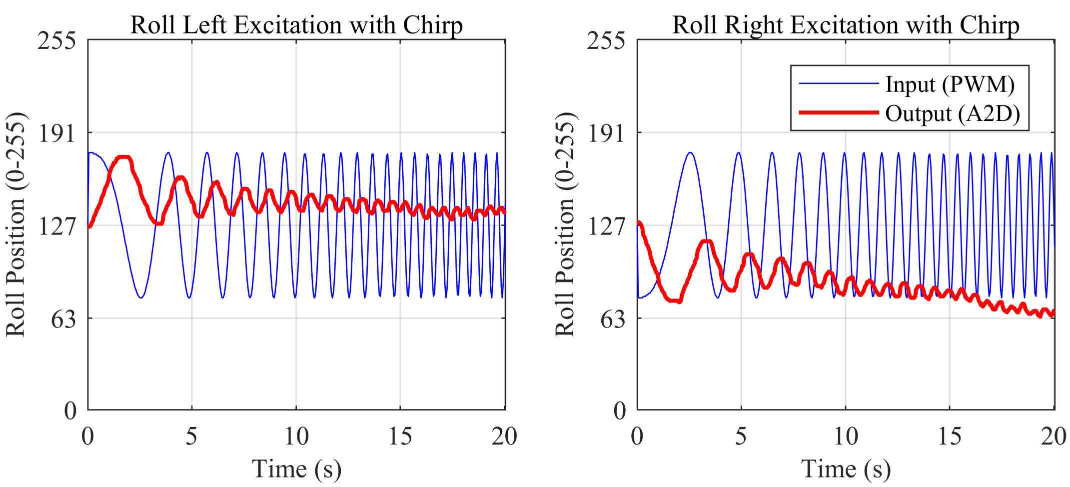

Figure 5. Open loop roll response to chirp excitation

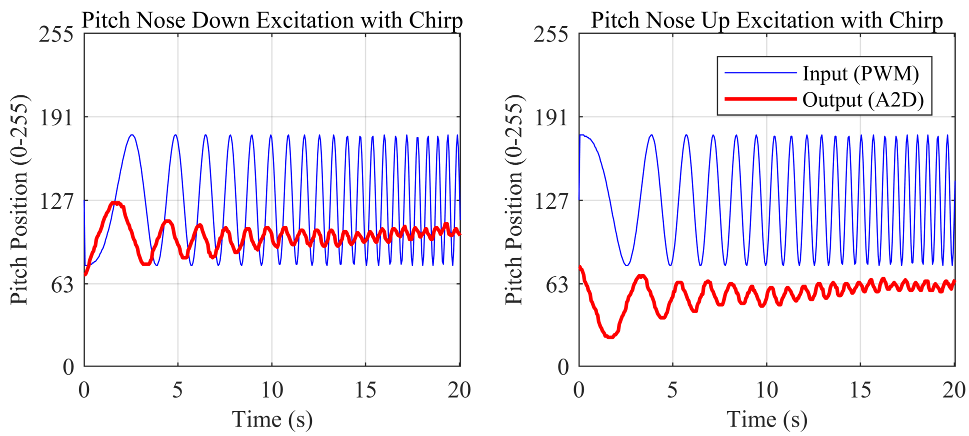

Figure 6. Open loop pitch response to chirp excitation

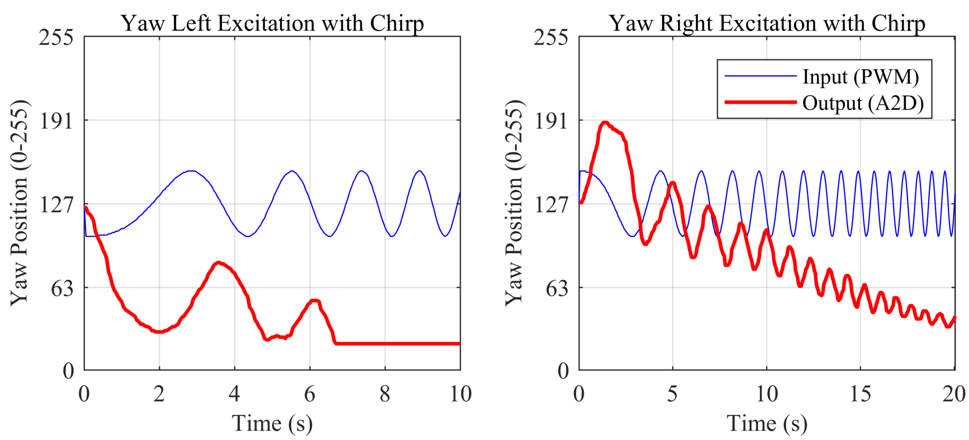

Figure 7. Open loop yaw response to chirp excitation

The ARX models that fit the above estimation data are stated as

$$G_{\varphi}(z) = \frac{-0.02129 + 0.05437z^{-1}}{1 - 0.9935z^{-1} - 0.1025z^{-2} + 0.09543z^{-3}} \tag{13}$$

$$G_{\theta}(z) = \frac{0.01277 - 0.04207z^{-1}}{1 - 1.003z^{-1} - 0.02931z^{-2} + 0.03222z^{-3}} \tag{14}$$

$$G_{\psi}(z) = \frac{-0.002453 + 0.02788z^{-1}}{1 - 1.404z^{-1} + 0.1334z^{-2} + 0.2704z^{-3}} \tag{15}$$

Further data was collected to validate the identified systems. The signal used to validate the models was chosen to contain sinusoids spanning frequencies present in the training data. The frequencies and amplitudes of the input signal were chosen to be similar to that of which would be observed in real flight. Figures 8 through 10 show the measured response as compared to the simulated response of the identified model for the chosen input signal.

As seen in Fig. 8 and Fig. 9, the simulated responses of the identified roll and pitch models closely match the measured responses. However, as evident in the open loop yaw response (Fig. 7) and the validation data (Fig. 10), yaw exhibits mechanical limitations, such as asymmetry in the motor and slack in the yaw mechanism, that make the platform an undamped, sprung mass. This non-linearity and physical limitation

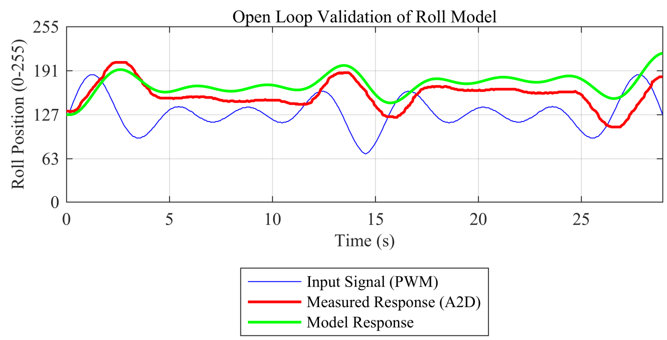

Figure 8. Open loop validation of platform roll

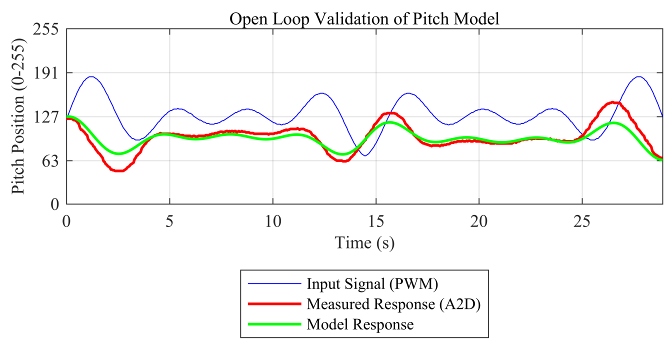

Figure 9. Open loop validation of platform pitch

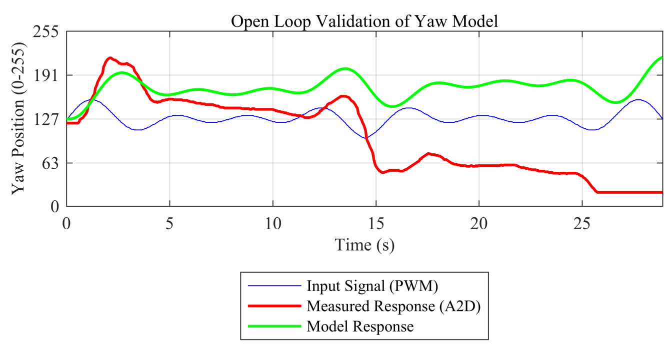

Figure 10. Open loop validation of platform yaw

degrade the accuracy of estimates of the model, but not its utility in controller design.

III. Control of Simulator Platform

III.A. Architecture

The controller architecture follows the typical PID architecture as shown in Figure 11. All signals depicted

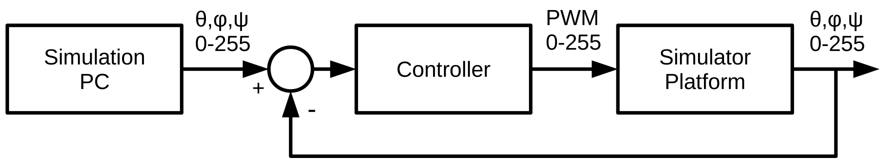

Figure 11. Block Diagram of CCSU Flight Simulator

in the controller block diagram are represented by eight bit values (0-255). This representation is consistent with the output of the driver written by CCSU faculty and students to translate UDP packets from X-plane and the serial input to the control electronics described in previous work. This driver software performs all scaling of measurements to the equivalent reference value for the platform. The controller and measurement of actuator position was implemented on an eight bit microcontroller eliminating the need to further scale any of the signals.

The controller implements two additional features typical to practical PID controllers. First, anti-integral windup prevents the integral term from accumulating a large error and causing excessive overshoot. For all three controllers the saturation limits were set to ± 20. This limit is large enough to allow the integral term to overcome the dead-band of the motors while preventing integral windup.

Second, the derivative term is high pass. Any noise present in the system will be aliased during discretization. The controller implements an additional discrete filter in the form on an infinite impulse response (IIR) filter. The IIR results in an exponential moving average removing frequencies that would otherwise interfere with operation of the controller.

III.B. Selection of Gains and System Characteristics

The gains implemented in the controller were chosen for a balance of reference tracking and disturbance rejection. The gains for roll, pitch, and yaw were selected to achieve an over-damped system with minimal response time while keeping proportional gains small enough to mitigate the effect of measurement noise. For roll and yaw, the proportional and integral terms were sufficient. For pitch, the derivative term was added with a first-order filter with time constant, τ_f. The model gain selection and step response characteristics are detailed in Table 1.

	Gains	Rise Time	Settling Time	Overshoot
Roll	$K_p = 5$, $K_i = 0.2$	0.4195 s	1.0137 s	0%
Pitch	$K_p = 6$, $K_i = 0.2$, $K_d = 0.239$, $\tau_f = 0.077$	0.7941 s	1.0088 s	0%
Yaw	$K_p = 1.83$, $K_i = 0.05$	0.6877 s	1.0117 s	0%

Table 1. System characteristics

III.C. Validation of Closed-Loop Response

The simulation PC was programmed to provide two signals for validation of the closed-loop responses of all three axes. The first signal was a chirp. The model and estimated parameters indicate a low-pass response of the closed-loop system. The chirp reference confirms this. As the frequency increases beyond the system's cut-off frequency, the attenuation and phase-shift anticipated was observed. Figures 12 through 14 display the platform response to the chirp signals.

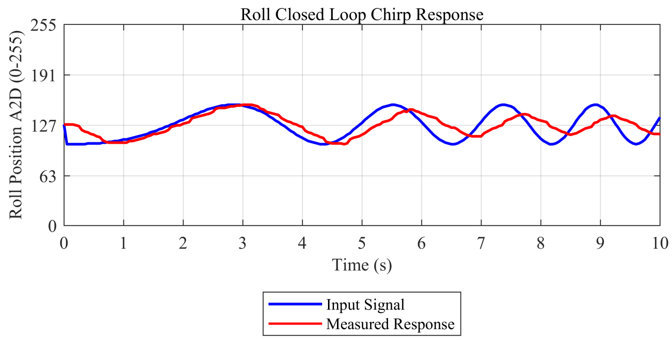

Figure 12. Closed loop validation of roll with chirp

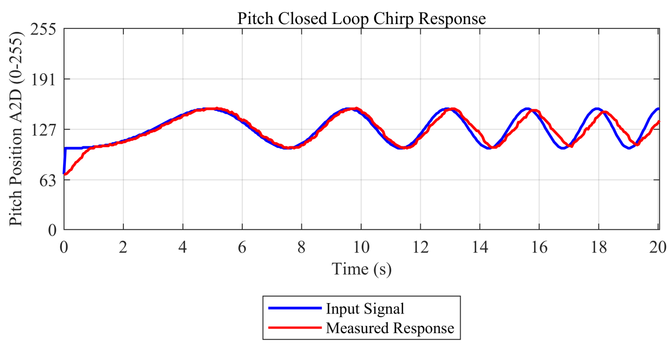

Figure 13. Closed loop validation of pitch with chirp

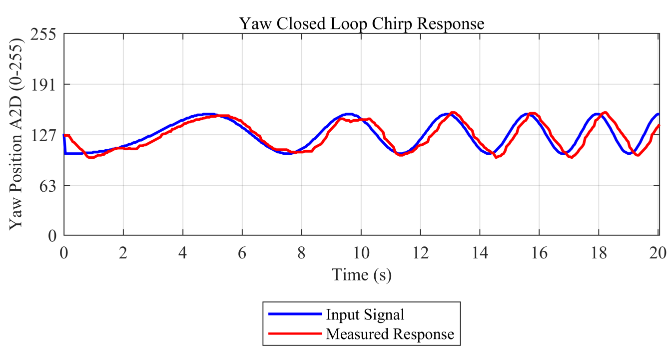

Figure 14. Closed loop validation of yaw with chirp

The chirp reference signal deliberately pushed the platform past its ability to track the reference. The simulation PC was also programmed to provide a reference more typical of helicopter flight. Figures 15 through 17 display the platform response to this signal for all three axes.

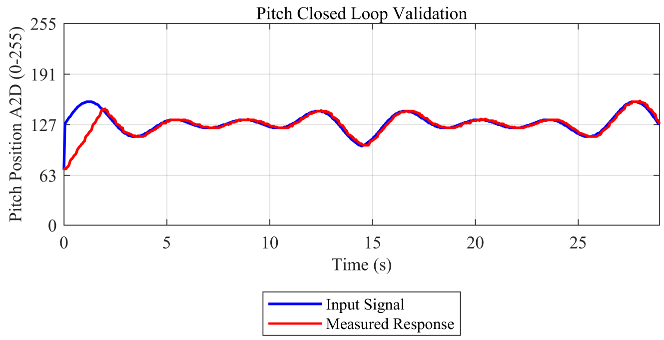

Figure 15. Platform roll position tracking of typical reference during flight

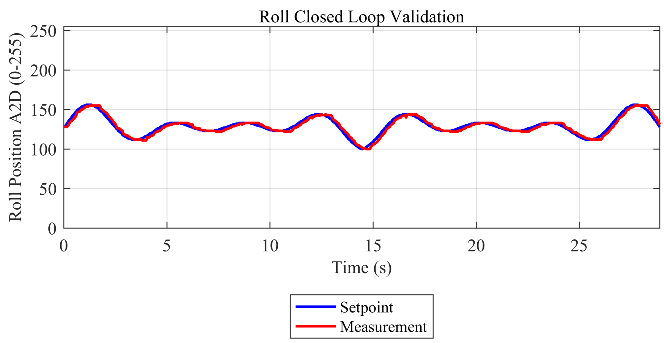

Figure 16. Platform pitch position tracking of typical reference during flight

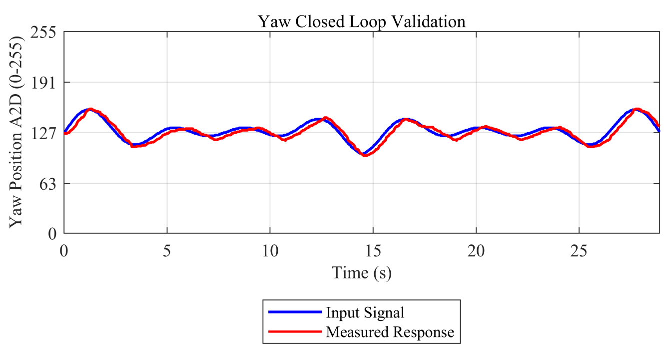

Figure 17. Platform yaw position tracking of typical reference during flight

This group of plots demonstrates that the models identified as part of this work, while not accurate for simulation in some cases, are useful in controller design. The selected gains cause the closed loop system to track the reference in a manner that will be adequate for novice pilot training.

IV. Characterization of Flight Capabilities

As anticipated, the closed loop validation revealed the limitations of the simulator platform. The chirp reference signal shows the limitations of each axis motor in a manner typical of a linear system. Above the cut-off frequency the output of the systems will display attenuation and phase shift, both undesirable for this work.

In addition to the linear limitations of the system there are additional nonlinear effects that were considered. The voltage limit of the motors creates a nonlinear saturation. The motors and gearboxes limit the magnitude of force that can be applied to the platform. This limitation became apparent during data collection for the closed loop validation and, subjectively, during use of the simulator.

The first seconds of Fig. 12 through Fig. 14 show the platform position converging on the tracking signal. In each plot the platform was not positioned on the initial value of the reference. As the error was large, the control effort reached the saturation caused by the voltage limit. This saturation proved to be the limiting factor in the platforms ability to match some angular rates indicated by the X-Plane reference signals. Table 2 summarizes these rate limitations. This limitation was also apparent in the flight maneuvers

	Positive	Negative
Roll	16.99 $^{deg}/_{s}$	16.06 $^{deg}/_{s}$
Pitch	11.63 $^{deg}/_{s}$	11.80 $^{deg}/_{s}$

Table 2. Summary of platform rate limitations

to be presented in subsequent sections. The platform was capable of tracking small changes in reference; those present during a hover or low rate turn. The platform was not able to track larger jogs in the reference creating a lagging sensation for the pilot. The extent of this lag is apparent in the data presented in the next section.

V. Flight Data

A novice pilot attempted a number of maneuvers in the simulator to examine the platform response under typical flight conditions. A Sikorsky S-61 Sea King provided a suitable aircraft for an inexperienced pilot. The pilot performed the maneuvers detailed below while the simulation PC recorded the setpoints and measurements for all three axes. The targeted maneuvers range from basic to advanced flight maneuvers detail in the literature.[28,29]

V.A. Hover

The student pilot began with hovering flight over a fixed reference with the goal of maintaining a constant altitude and heading. Figure 18 shows the recorded data during this hovering maneuver. The data shows an 18 s period of flight in which the helicopter maintained position. The subtle movements of the platform matched those of the simulated helicopter for the roll and pitch axes. The yaw axis demonstrates lag when moving in the positive direction. This lag is consistent with the open and closed loop validation plot presented above.

V.B. Hovering to Forward Flight

The student pilot attempted to transition from hovering flight to forward flight. Every endeavor was made to maintain constant ground speed, altitude, and heading once in forward flight. Figure 19 shows the recorded

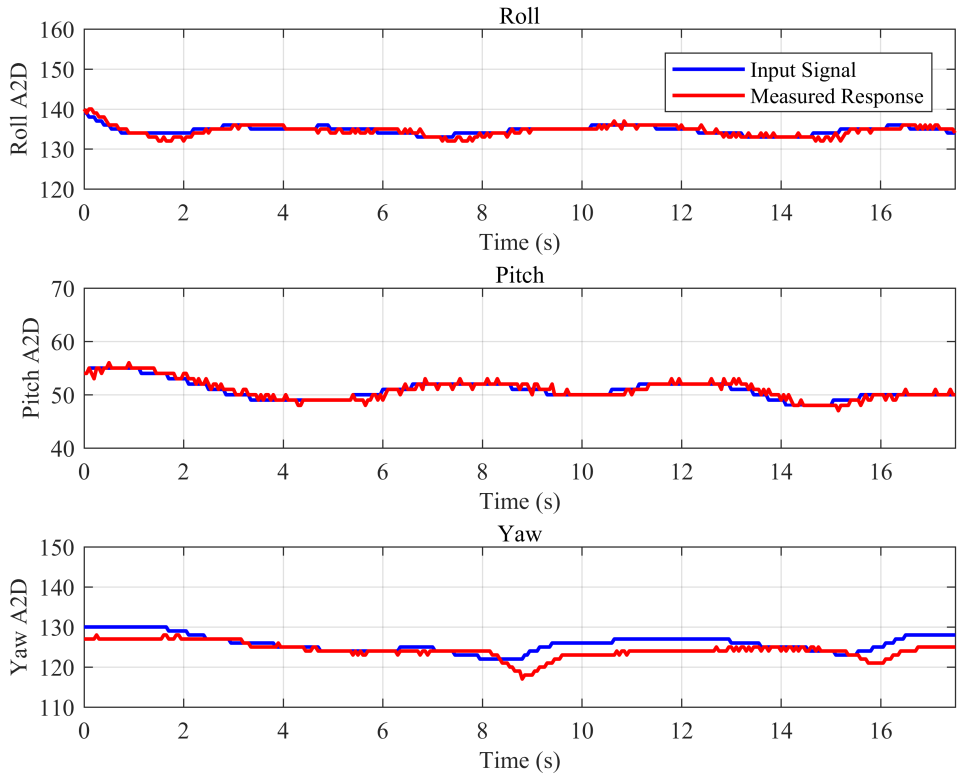

Figure 18. Flight data during hover maneuver

pitch angle during the transition to forward flight. Roll and yaw were held near constant and are not displayed. The student pilot began with the nose pitched up and proceed to push the cyclic forward. The reference for the platform indicates that the nose was commanded down. The measured value of platform pitch shows lag during this large transient. This is consistent with the limitations identified in previous sections. The return to level flight shows the platform tracked the reference through smaller transient maneuvers within the identified limitations.

V.C. Hovering to Sidewards Flight

The student pilot attempted to transition from hovering flight to sidewards flight. Every endeavor was made to maintain constant ground speed, altitude, and heading once in sidewards flight. Figure 20 shows the recorded roll angle during the transition to sidewards flight. Pitch and yaw were held near constant and are not displayed. The platform can roll from -45° to 45°. During this maneuver both limits were exercised and can be seen in the measured data. The jog from one limit to the other that begins at 17 s demonstrates the limited roll rate of the platform as discussed above.

V.D. Hovering Turns

The student pilot attempted to turn while in hovering flight. Every endeavor was made to maintain constant ground speed, altitude, pitch, and roll. Figure 21 shows the recorded yaw angle of the platform during the turns. Pitch and roll were held near constant and are not displayed.

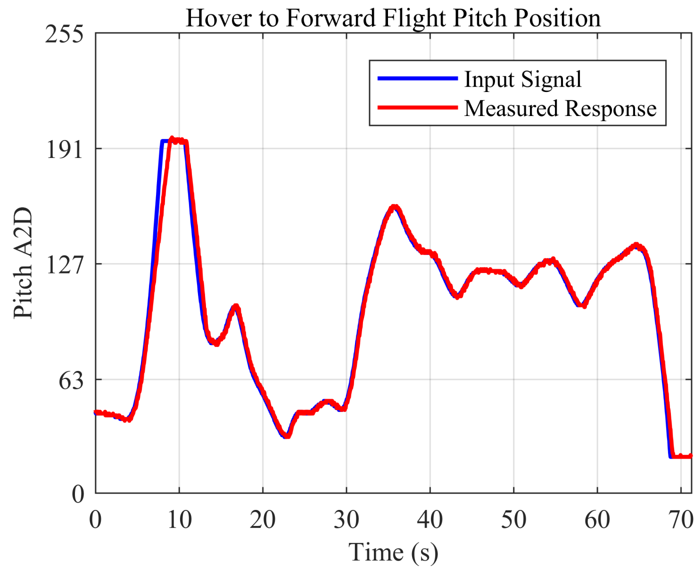

Figure 19. Flight data during hover to forward flight

Figure 20. Flight data during hover to sidewards flight

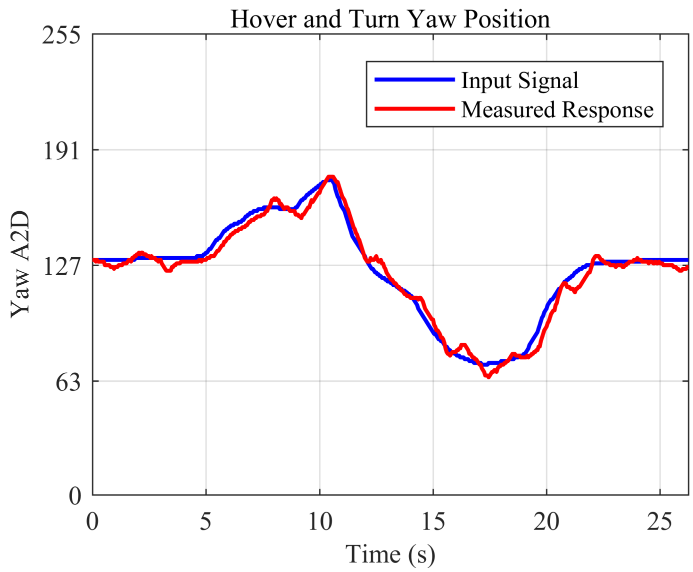

Figure 21. Flight data during a hover and turn

It is evident in this plot that the controller does track the reference. However, the platform does not track the reference smoothly. The identified model assumes that the platform is a rigid body rotating around a fixed point. The yaw axis is more accurately described by a sprung mass rotating on top of the rigid platform. In addition, the asymmetry discussed early contributes to the poor tracking of the reference. In spite of these deficiencies the controller does cause the platform to track the reference in a subjectively adequate manner.

VI. Conclusion

This paper presented the system identification, controller tuning and validation, and comparison of simulator dynamics against an available helicopter dynamic model during typical flight maneuvers.

Model order was determined through physical principles and clearly stated assumptions. The performance of the roll and pitch models was acceptable in open loop simulation. The performance of the yaw model demonstrated that assumptions were not valid for this axis. While this model was not accurate for simulation it proved useful in the selection of gains for the controller.

In fact, all three axis models proved useful in the selection of gains. Gains were selected to balance reference tracking and response time and were validated with data collection on the platform itself. All three axes closely tracked the reference signal in closed loop operation.

The limitations of the platform rotational rates were identified and quantified using recorded data. These limitations were evident in validation maneuvers as well as flight maneuvers performed by a novice pilot. The platform was shown to track the reference signals during hover, hover to forward flight, hover to sidewards flight, and hovering turns. Deviations from the reference signal were observed during larger jogs. However, more typical motions of a helicopter were accurately recreated by the platform providing valuable feedback to the pilot.

References

[1]Wei, F. and Gallagher, F., "K-MAX Rotor Blade Flight Loads Survey For Out of Envelope Flight Test," *ANNUAL FORUM PROCEEDINGS-AMERICAN HELICOPTER SOCIETY*, Vol. 64, AMERICAN HELICOPTER SOCIETY, INC, May 1 2008, p. 574.

[2]Gallagher, F., Wei, F., and Gates, A., "Kaman K-MAX K-1200 high altitude performance," *AHS International, 58 th Annual Forum Proceedings-*, Vol. 1, 2002, pp. 1063–1070.

[3]Wei, F. and Gallagher, F., "The Servo-Flap Rotor and Aircrew Survivability," *ANNUAL FORUM PROCEEDINGS-AMERICAN HELICOPTER SOCIETY*, Vol. 62, AMERICAN HELICOPTER SOCIETY, INC, 2006, p. 174.

[4]Wei, F. and Peters, D., "Systematic Analysis of Rotor Blade Effective Twist Due to Platform Variation," *The 71st American Helicopter Annual Forum*, Virginia Beach, Virginia, May 5-7 2015.

[5]Peddireddy, K., *Structure Safe Design Factor for CCSU Flight Simulator*, Master's thesis, CCSU, Department of Engineering, January 2015.

[6]Coppola, Z., Root, J., and Rose, D., "Helicopter Flight Simulator Project - Senior Project I & II," Tech. rep., CCSU Department of Engineering, December 2014.

[7]Pinciaro, A., Coelho, T., and Akach, A., "Helicopter Flight Simulator Mechanical Control & Software Application," Tech. rep., CCSU Department of Engineering, May 2014.

[8]Gessow, A. and Myers, G. C., *Aerodynamics of the Helicopter*, Frederick Ungar, 1952.

[9]Wei, F.-S., Moore, E., and Gates, A., "An Intermeshing Rotor Helicopter Design and Test," *The AIAA SciTech 2015 Conference, Kissimmee, Florida*, 2015.

[10]Johnson, W., *Helicopter theory*, Princeton University Press, 1980.

[11]Saunders, G. H., *Dynamics of helicopter flight*, John Wiley & Sons, 1975.

[12]Wei, F., Gates, A., and Vasko, T., "Identification of High Speed Rotating Rotor Blades," *IMAC-XXXI Conference & Exposition on Structural Dynamics, Garden Grove, California*, 2013.

[13]Wei, F.-S., "Active trailing edge tab control for helicopter rotor vibration reduction," *AIAA Dynamics Specialists Conference, dated*, Vol. 18, 1996.

[14]Wei, F.-S. and Gunsallus, C., "A New Approach to Rotor Blade Performance Design Improvement," *The 48th AIAA/ASME/ASCE/AHS/ASC Structures, Structure Dynamics and Material Conference, Honolulu, Hawaii*, 2007.

[15]Muzsi, I., Angelotti, P., and LaFlesh, P., "Helicopter Flight Simulator Motion Platform Design & Manufacture," Tech. rep., CCSU Department of Engineering, 2012.

[16]Davis, J., Maida, E., Nguyen, N., Richard, E., Wheatley, L., and Yardito, T., "Helicopter Flight Simulator," Tech. rep., CCSU Department of Engineering, May 2013.

[17]Wei, F.-S., "Design of an integrated servo-flap main rotor," *ANNUAL FORUM PROCEEDINGS-AMERICAN HELICOPTER SOCIETY*, Vol. 59, AMERICAN HELICOPTER SOCIETY, INC, 2003, pp. 603–613.

[18]Lago, S., Taylor, D., and McIntyre, G., "Helicopter Flight Simulator Development and Modification," Tech. rep., CCSU, May 2016.

[19]Ciccio, J. and Bufalini, M., "Helicopter Flight Simulator Electrical Design," Tech. rep., CCSU Computer Electronics and Graphics Technology Department, May 2016.

[20]Giansante, N., "Advanced Rotor Actuation Methods (ARAM)," Tech. rep., USAATCOM TR 95-D-10, 1996.

[21]Fulton, M. V. and Ormiston, R. A., "Small-scale rotor experiments with on-blade elevons to reduce blade vibratory loads in forward flight," *Proceedings of the 54th Annual Forum of the American Helicopter Society*, 1998, pp. 433–451.

[22]Straub, F. and Charles, B., "Preliminary assessment of advanced rotor/control system concepts (arcs)," *McDonnell Douglas Helicopter Co., Aviation Applied Technology Directorate, US Army Aviation Systems Command, Fort Eustis, VA, USAAVSCOM TR*, 1990.

[23]Phillips, N. B. and Merkley, D. J., "BHTI's technical assessment of advanced rotor and control concepts," *Vertical Lift Aircraft Design Conference, San Francisco, CA, Proceedings*, Vol. 17, 1990.

[24]Wei, F.-S. and Jones, R., "Dynamic tuning of the SH-2 F composite main rotor blade," *AHS, Annual Forum, 43 rd, Saint Louis, MO, Proceedings.*, Vol. 2, 1987, pp. 527–537.

[25]Wei, F.-S., Basile, J. P., and Jones, R., "Vibration reduction on servo flap controlled rotor using hhc," *AHS National Specialists' Meeting on Rotorcraft Dynamics, Arlington, TX, Proceedings*, Vol. 13, 1989.

[26]Wei, F.-S., Amaya-Bower, L., Gates, A., Rose, D., and Vasko, T., "The Full-Scale Helicopter Flight Simulator Design and Fabrication at CCSU," *57th AIAA/ASCE/AHS/ASC Structures, Structural Dynamics, and Materials Conference*, 2016, p. 0582.

[27] Broderick, D. J., Wei, F.-S. J., Ciccio, J., and Bufalini, M., "Electronic Controller Design and Fabrication for Full-Scale Helicopter Flight Simulator at CCSU," *55th AIAA Aerospace Sciences Meeting*, 2017, p. 0301.

[28] Helicopter Flight Handbook, "FAA-H-8083-21A," .

[29] Tang, J., Singh, A., Goehausen, N., and Abbeel, P., "Parameterized maneuver learning for autonomous helicopter flight," *Robotics and Automation (ICRA), 2010 IEEE International Conference on*, IEEE, 2010, pp. 1142–1148.